Conjugated Polymers with Broad Absorption: Synthesis and Application in Polymer Solar Cells

JINSHENG SONG,[1] CHI ZHANG,[1] CUIHONG LI,[1,2] WEIWEI LI,[1] RUIPING QIN,[2] BINSONG LI,[1] ZHENGPING LIU,[2] ZHISHAN BO[1,2]

[1]Institute of Chemistry, Chinese Academy of Sciences, Beijing 100190, China

[2]College of Chemistry, Beijing Normal University, Beijing 100875, China

ABSTRACT: A series of main chain donor-acceptor low-bandgap conjugated polymers were designed, synthesized, and used for the fabrication of polymer solar cells. The absorption spectra of low-bandgap conjugated polymers were tuned by the ratio of three copolymerization monomers. The polymers in films exhibited broad absorption ranging from 300 to 1000 nm with optical bandgaps of around 1.40 eV. All of the polymers have been investigated as an electron donor in photovoltaic cells blending with PCBM ([6, 6]-phenyl C61-butyric acid methyl ester) as an electron acceptor and power conversion efficiencies (PCEs) of 1.32–1.8% have been obtained. As for **P1**, PCE increases from 1.67 to 2.44% after adding 1,8-diiodooctane as an additive. The higher PCEs are probably because of better phase separation of blend films. © 2010 Wiley Periodicals, Inc. J Polym Sci Part A: Polym Chem 48: 2571–2578, 2010

KEYWORDS: conjugated copolymers; photovoltaic; polycondensation; solar cells; structure-property relations; Suzuki–Miyaura–Schlüter

INTRODUCTION Recently, polymer solar cells (PSCs) have attracted great interest because of the prospect of low-cost, lightweight, and potential applications in large-area flexible devices.[1–10] Great efforts have been devoted to improve the power conversion efficiency (PCE) of PSCs by the design and synthesis of new low-bandgap polymer materials. Several new low-bandgap conjugated polymers with the main chain alternating donor-acceptor structure have been developed and used in PSCs, and their PCEs are higher than 5%.[11–13] More recently, PCE of 6.5% has been attained,[14] which is very promising for the future of PSCs.

Poly(3-hexylthiophene) (P3HT) is a widely used *p*-type conjugated polymer in the field of polymer photovoltaics. However, the bandgap of P3HT is higher than 2.0 eV (600 nm) and its absorption bandwidth is too narrow to absorb a large fraction of the solar spectrum.[3] The mismatch between absorption spectra of the conjugated polymers and the solar spectrum is one of the main reasons for the low PCE of PSCs. The fabrication of tandem solar cell and the use of broad absorption polymer/PCBM blends as the active layer are two main strategies to make PSCs better match the solar spectrum. Tandem solar cells[15] are two single layer bulk heterojunction cells stacked in series, each layer with a different absorption region, and the combined absorption covers a broader region of the solar spectrum. However, the fabrication of tandem solar cell requires more complicated procedure than the buildup of a single layer one. Development of new broad absorption conjugated polymers becomes extremely important to achieve high-efficiency PSCs. Recently, conjugated copolymers with a main chain alternating donor-acceptor (D-A) structure have attracted considerable attention because of their broad absorption and higher PCE.[6,16–28] Many low-bandgap polymers have been prepared and used for PSCs, including APFO-3,[18,19] PSBTBT,[10] PSiF-DBT,[23] PCD-TBT,[20] PCPDTBT,[22] HXS-1,[11] and APFO-Green-1.[29] According to their absorption spectra, the aforementioned polymers can be divided into two categories. The first category, comprising APFO-3, PCDTBT, PSiF-DBT, and HXS-1, exhibits two strong absorption bands in the visible region peaked at about 380 and 550 nm, respectively. The second one, including PSBTBT, APFO-Green-1, and PCPDTBT, exhibits two strong absorption bands peaked at about 420 nm and 700–850 nm, respectively. The absorption spectra of these two categories do not match the solar spectrum very well. The first category lacks the long wavelength absorption in the NIR region. For the second category with APFO-green-1 as an example, the absorption of polymers in the region of about 500–600 nm is relatively weak.

To better match the solar spectrum, we report here the design and synthesis of new broad absorption polymers for high-efficiency solar cells. As shown in Scheme 1, the main chain of broad absorption conjugated polymers is composed of three kinds of functional building blocks, namely, 6,7-dioctyl-4,9-di(thiophen-2-yl)-[1,2,5]thiadiazolo[3,4-g]quinoxaline,
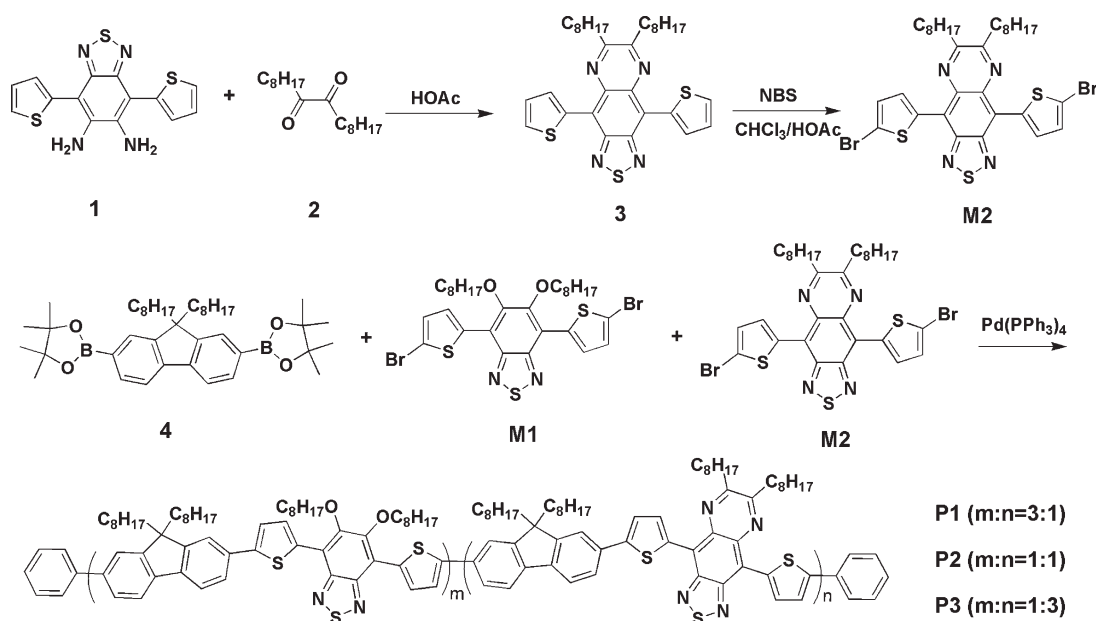
SCHEME 1 Synthetic routes to monomer **M2** and Polymers **P1–3**.

5,6-bis(octyloxy)-4,7-di(thiophen-2-yl)benzo[c][1,2,5]thiadiazole, and 9,9-dioctylfluorene. Copolymers **P1–3**, which exhibit three broad absorption peaks in the range of 300–1000 nm, were prepared by Suzuki–Miyaura–Schlüter polycondensation of three monomers (*vide infra*). The relative intensity of three absorption peaks can be effectively tuned by the fed ratio of these monomers. Photovoltaic devices based on polymer/$PC_{61}BM$ blends were fabricated by spin-coating from dichlorobenzene (DCB). Without additive, device based on polymer **P2** demonstrates high-performance with PCE of 1.8%. With 1,8-diiodooctane as an additive, device based on polymer **P1** shows the best PCE of 2.4%. Comparing with APFO-green 1, increasing of absorption range of polymers can effectively increase the PCE of solar cells.

EXPERIMENTAL

Materials and Instruments
All reagents were purchased from commercial suppliers and used without further purification unless otherwise indicated. Compounds **1**,[29] **2**,[30] **4**,[31] and 4,7-bis(5-bromothiophen-2-yl)-5,6-bis(octyloxy)benzo[c][1,2,5]thiadiazole (**M1**)[11] were prepared by following the literature procedures. The catalyst precursor $Pd(PPh_3)_4$ was prepared, according to the literature,[32] and stored in a Schlenk tube under nitrogen. Tetrahydrofuran (THF) and toluene was distilled from Na under nitrogen with benzophenone as an indicator. Thin-layer chromatography analysis was performed using silica gel HSG (F254) plates, and the eluted plates were observed under a UV detector. Chromatographic purifications were performed by flash chromatography on silica gel (200–300 mesh). ^1H and ^{13}C NMR spectra were recorded on a Bruker AV400 spectrometer with choroform-d_1 as the solvent. UV–visible absorption spectra were recorded on a UV-1601pc spectrometer. Matrix-assisted laser desorption ionization time of flight (MALDI-TOF) mass spectra were recorded on a BIFLEXIV

mass spectrometer. Elemental analysis was performed on a Vario EL elemental analysis instrument. Number-(M_n) and weight-average (M_w) molecular weights were measured by gel permeation chromatography (GPC) on a Waters GPC2410 with THF as an eluent and calibrated with polystyrene standards. Atomic force microscopy (AFM) images of blend films were obtained on a Nanoscope IIIa Dimension 3100 operating in the tapping mode. Thermogravimetric analysis (TGA) was performed on a Perkin-Elmer Pyris 1 analyzer under a nitrogen atmosphere (100 mL/min) at a heating rate of 10 °C/min. Differential scanning calorimetry (DSC) measurements were performed on a Mettler Toledo DSC 822e with a heating and cooling rate of 20 °C/min. Electrochemical measurements were performed on a CHI 630A electrochemical analyzer.

Fabrication and Characterization of PSCs
PSCs were fabricated with the device configuration of ITO/PEDOT:PSS/active layer/Al. The conductivity of ITO was 20 Ω/□ and PEDOT:PSS is Baytron P VP.AI 4083. A thin layer of PEDOT:PSS was spin coated on top of cleaned ITO substrate at 2400 rpm/s and dried subsequently at 120 °C for 10 min on a hotplate before transferred into a glove box. The active layer was prepared by spin-coating the 1,2-dichlorobenzene solution of polymers and $PC_{61}BM$ on the top of ITO/PEDOT:PSS. The thickness of the active layers was characterized by AFM using a tapping mode. The top electrode was thermally evaporated a 100 nm of aluminum at a pressure of 10^{-6} Torr through a shadow mask. Eight OSCs were fabricated on one substrate and the effective area of one cell is 4 mm^2. The characterization of solar cell devices was carried out on a computer controlled Keithley 236 digital source meter with an AM 1.5 solar simulator (Oriel model 96,000) (100 mW/cm^{-2}) as the light source.

Monomer Synthesis

6,7-dioctyl-4,9-di(thiophen-2-yl)-[1,2,5]thiadiazolo[3,4-g]quinoxaline (3)

To a slurry of 4,7-di(thiophen-2-yl)benzo[c][1,2,5]thiadiazole-5,6-diamine (1) (1.04 g, 3.1 mmol), in acetic acid (100 mL), was added octadecane-9,10-dione (1.78 g, 6.3 mmol). The mixture was stirred at room temperature for 24 h and then partitioned between diethyl ether (100 mL) and water (150 mL); the organic layer was separated, washed with water for three times (3 × 100 mL), dried over anhydrous Na_2SO_4, and evaporated to dryness; and the residue was chromatographically purified on a silica gel column eluting with CH_2Cl_2/hexane (1:12, v/v) to afford 3 as a dark blue powder (1.18 g, 65%). ^{1}H NMR (400 MHz, CDCl$_3$): δ 8.95 (d, 2H), 7.62 (d, 2H), 7.28 (t, 2H), 3.07 (t, 4H), 2.04 (p, 4H), 1.55–1.26 (m, 20H), 0.9 (t, 6H). ^{13}C NMR (100 MHz, CDCl$_3$): δ 157.4, 151.4, 136.0, 135.1, 132.8, 130.8, 126.7, 121.0, 35.6, 32.1, 29.8, 29.7, 29.4, 28.30, 22.9, 14.3. MALDI-TOF MS: m/z calcd for $C_{32}H_{40}N_4S_3$ 576.2, Found 577.4. HRMS (EI, M+): m/z Calcd for 576.2415, Found 576.2418.

4,9-bis(5-bromothiophen-2-yl)-6,7-dioctyl-[1,2,5]thiadiazolo[3,4-g]quinoxaline (M2)

To a solution of compound 3 (1.18 g, 2.0 mmol) in a solvent mixture of chloroform (80 mL) and acetic acid (80 mL), was added NBS (0.74 g, 4.16 mmol) in darkness. The mixture was stirred at room temperature for 3 h. Acetic acid was removed by extraction and the residue was purified by chromatography on silica gel eluting with CH_2Cl_2/hexane (1:8, v/v) and then Soxhlet extraction with methanol for 24 h. The product was obtained as a dark-blue powder (1.2 g, 80%). ^{1}H NMR (400 MHz, CDCl$_3$): δ 8.84 (d, 2H), 7.21 (d, 2H), 3.06 (t, 4H), 2.02 (p, 4H), 1.51-1.34 (m, 20H), 0.9 (t, 6H). ^{13}C NMR (100 MHz, CDCl$_3$): δ 157.7, 150.8, 137.5, 134.5, 133.1, 129.6, 120.2, 120.0, 35.7, 32.2, 29.9, 29.8, 29.5, 28.3, 22.9, 14.4. MALDI-TOF MS: m/z calcd for $C_{32}H_{38}Br_2N_4S_3$ 734.1, Found 734.2. Anal. Calcd for $C_{32}H_{38}Br_2N_4S_3$: C, 52.31; H, 5.21; N, 7.63. Found: C, 51.91; H, 5.06; N, 7.75.

General Procedures for the Synthesis of Polymers 1–3 Using Suzuki–Miyaura–Schlüter Polycondensation

A mixture of M1, M2, 4,4,5,5-tetramethyl-2-(2-(4,4,5,5-tetramethyl-1,3,2-dioxaborolan-2-yl)-9,9-dioctyl-9H-fluoren-7-yl)-1,3,2-dioxaborolane (4), NaHCO$_3$ (0.6 g, 71.4 mmol), H$_2$O (3 mL), toluene (5 mL) and THF (20 mL) was carefully degassed before and after 3 mg Pd(PPh$_3$)$_4$ was added. The mixture was stirred and refluxed for 19 h under nitrogen atmosphere. Phenylboronic acid (10 mg, 0.08 mmol) was added; the reaction was further refluxed for 1 h; then 1-bromobenzene (0.05 mL, 0.48 mmol) was added; and the reaction was refluxed for another 1 h. The reaction mixture was then allowed to cool to room temperature, the whole reaction mixture was poured into acetone (200 mL), and the resulted precipitate was collected by filtration. The crude polymer was dissolved in hot chloroform (300 mL) and filtered. The filtration was concentrated to about 100 mL and precipitated into acetone (400 mL). The precipitate was collected by filtration and dried under high-vacuum to afford the aimed polymer.

P1 (m:n = 3:1)

M1 (140.6 mg, 0.197 mmol), M2 (48.2 mg, 0.0656 mmol), and compound 4 (169.4 mg, 0.264 mmol) were used. P1 was obtained as a dark solid (214 mg, 86%). M_w and PDI measured by GPC calibrated with polystyrene standards are 46.3 kg/mol and 1.78, respectively. ^{1}H NMR (400 MHz, CDCl$_3$): δ 9.1(br), 8.59 (br), 7.76 (br), 7.56 (br), 4.25 (br), 3.11 (br), 2.08 (br), 1.58–0.81 (m, br) ^{13}C NMR (100 MHz, CDCl$_3$): δ 152.0, 151.2, 146.6, 140.7, 133.7, 133.7, 133.6, 133.6, 132.2, 125.2, 123.2, 123.1, 120.5, 120.4, 120.3, 117.8, 74.8, 55.6, 40.8, 32.4, 32.1, 32.0, 30.9, 30.7, 30.6, 30.4, 30.2, 29.9, 29.6, 29.5, 26.4, 24.1, 22.9, 22.8, 14.4, 14.3. Anal. Calcd. for $(C_{59.5}H_{80}N_{2.5}S_{2.25}O_{2.25})_n$: C, 75.18; H, 8.49; N, 3.67. Found: C, 74.88; H, 8.19; N, 3.49.

P2 (m:n = 1:1)

M1 (83 mg, 0.116 mmol), M2 (85 mg, 0.116 mmol), and compound 4 (149.4 mg, 0.233 mmol) were used. P2 was obtained as a dark solid with a yield of 58%. M_w and PDI measured by GPC calibrated with polystyrene standards are 17.9 and 1.67 kg/mol, respectively. ^{1}H NMR (400 MHz, CDCl$_3$): δ 9.1(br), 8.59 (br), 7.77 (br), 7.56 (br), 7.38 (br), 4.25 (br), 3.07 (br), 2.08 (br), 1.58–0.81 (m,br) ^{13}C-NMR (100 MHz, CDCl$_3$): δ 152.1, 152.0, 151.5, 151.2, 146.7, 146.6, 140.8, 140.7, 133.7, 133.6, 132.2, 129.0, 127.4, 125.2, 123.2, 120.4, 120.3, 117.8, 74.8, 55.6, 40.8, 40.7, 32.4, 32.1, 32.0, 30.8, 30.3, 30.1, 29.9, 29.7, 29.6, 29.5, 29.5, 26.4, 24.1, 24.0, 23.0, 22.9, 22.8, 14.4, 14.3, 14.2. Anal. Calcd. for $(C_{60}H_{80}N_3S_{2.5}O_{1.5})_n$: C, 75.42; H, 8.44; N, 4.38. Found: C, 75.21; H, 8.40; N, 4.54.

P3 (m:n = 1:3)

M1 (38.9 mg, 0.054 mmol), M2 (120 mg, 0.163 mmol), and compound 4 (140.6 mg, 0.219 mmol) were used. P3 was obtained as a dark solid (70 mg, 34%). M_w and PDI determined by GPC calibrated with polystyrene standards are 16.5 kg/mol and 1.94, respectively. ^{1}H NMR (400 MHz, CDCl$_3$): δ 9.1 (br), 8.59 (br), 7.78 (br), 7.62–7.57 (m, br), 7.38 (br), 4.26 (br), 3.15 (br), 2.09 (br), 1.59–0.81 (m, br). ^{13}C NMR (100 MHz, CDCl$_3$): δ 152.1, 152.0, 151.2, 140.8, 140.7, 133.7, 133.6, 132.2, 129.0, 127.4, 125.2, 123.2, 123.1, 120.6, 120.5, 120.4, 120.3, 120.2, 120.1, 74.8, 74.7, 55.6, 40.8, 32.5, 32.2, 32.1, 32.0, 32.8, 30.4, 30.3, 30.2, 29.9, 29.8, 29.6, 29.5, 29.5, 26.4, 23.0, 22.9, 22.8, 14.3, 14.2. Anal. Calcd. for $(C_{60.5}H_{80}N_{3.5}S_{2.75}O_{0.75})_n$: C, 75.65; H, 8.40; N, 5.09. Found: C, 74.45; H, 8.78; N, 4.45.

RESULTS AND DISCUSSION

Synthesis and Characterization

The syntheses of monomer M2 and polymers P1–3 are shown in Scheme 1. Starting from 4,7-di(thiophen-2-yl)benzo[c][1,2,5]thiadiazole-5,6-diamine (1),[29] its reaction with octadecane-9,10-dione (2)[30] in acetic acid at room temperature afforded 6,7-dioctyl-4,9-di(thiophen-2-yl)-[1,2,5]thiadiazolo[3,4-g]quinoxaline (3) in a yield of 65%. The bromination of compound 3 with NBS in a solvent mixture of chloroform and acetic acid at room temperature under dark furnished M2 in a yield of 80%. Polymers P1–3 were prepared by Suzuki–Miyaura–Schlüter polycondensation of dibromo
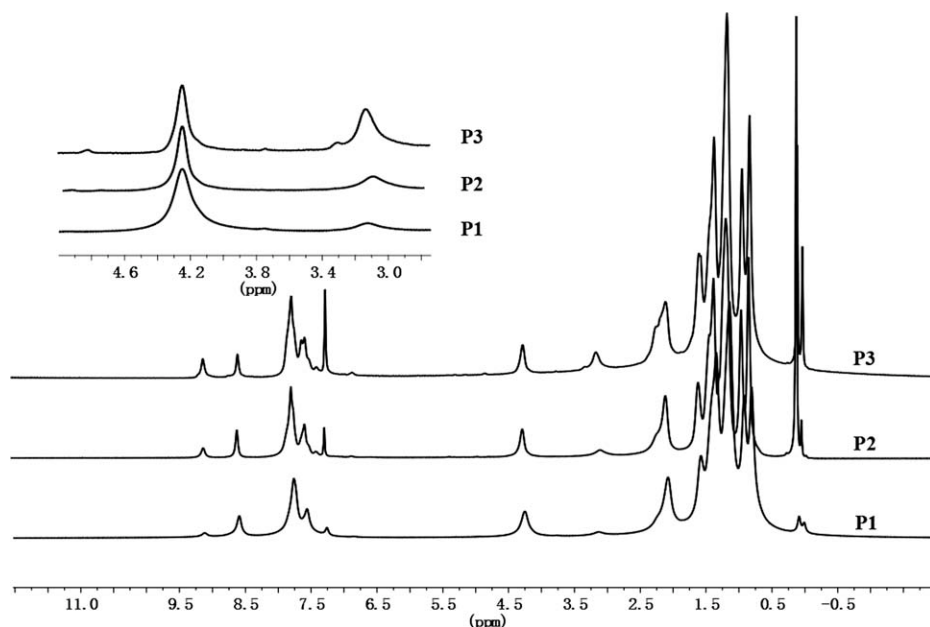
FIGURE 1 ^{1}H NMR spectra of polymers (**P1–3**).

monomers **M1** and **M2** with diboronic ester monomer **4** in a biphasic mixture of aqueous NaHCO$_3$ and THF/toluene (4:1, v:v) with freshly prepared Pd(PPh$_3$)$_4$ as the catalyst precursor. The feeding molar ratios of **M1** to **M2** are 3:1 for **P1**, 1:1 for **P2**, and 1:3 for **P3**. The chemical structures of **P1–3** were confirmed by ^{1}H NMR spectroscopy and the ^{1}H NMR spectra of **P1–3** are shown in Figure 1. The signals with chemical shifts of 4.3 and 3.1 ppm are assigned to protons of OCH$_2$ in benzo[c][1,2,5]thiadiazole units and CH$_2$ directly connected to [1,2,5]thiadiazolo[3,4-g]quinoxaline units, respectively. The integration ratio of these two peaks is equal to the feeding molar ratio of **M1** to **M2**, indication that the constitutions of polymers are consistent with the feeding monomers. Molecular weights and polydispersities of polymers determined by GPC against polystyrene standards are summarized in Table 1. Polymer **P1**, containing more benzo[c][1,2,5]thiadiazole fraction in the polymer main chain, displayed the highest molecular weight (M_n = 26,000). With the increasing of [1,2,5]thiadiazolo[3,4-g]quinoxaline fraction, M_n of polymers decreased to 10,700 for **P2** and 8500 for **P3**. With the increasing of [1,2,5]thiadiazolo[3,4-g]quinoxaline fraction, yields of polymers also decreased from 86% for **P1** to 58% for **P2**, and finally 34% for **P3**. The molecular weight of polymers is mainly determined by their solubility in the reaction media used for polymerization. All polymers precipitated from the reaction media during the polymerization, and could partially redissolve into chloroform at an elevated temperature.

The thermal properties of three polymers were investigated by TGA and the results are listed Table 1. All the three polymers possess good thermal stability with the decomposition temperature (5% weight loss) around 350 °C in nitrogen atmosphere. The high-thermal stability is crucial for the application in PSCs. No distinct glass transition was observed from 25 to 300 °C in their DSC curves of the second heating and cooling runs (20 °C/min).

Optical Properties

The normalized UV–vis–NIR absorption spectra of polymers (**P1–3**) in chloroform solution and films are shown in Figure 2. In solution, all the three polymers exhibit broad absorption in the region of 300–1000 nm with three peaks, two of them in the high energy region (320–480 nm and 480–600 nm) and the other one in the low-energy region (600–1000 nm). The absorption intensity of these peaks is related to the components of these polymers. The absorption peak at short wavelength (320–480 nm) originates from the π–π^* transition of fluorene units, whereas the region of 480–600 nm and 600–1000 nm can be attributed to the contribution of benzo[c][1,2,5]thiadiazole and [1,2,5]thiadiazolo[3,4-g]quinoxaline units, respectively. The relative intensity of the absorption peak at about 510 nm decreases with the decreasing of the content of benzo[c][1,2,5]thiadiazole unit; whereas the relative intensity of absorption at about 710 nm increases with the increasing of the content of [1,2,5]thiadiazolo[3,4-g]quinoxaline unit. Therefore, the absorption spectra of polymers can be easily tuned by the feeding molar ratio of **M1** to **M2**. Compared with their absorption spectra in solution, in films the three polymers exhibit slightly broader and red-shifted feature. For all three polymers, the relative intensity of the low-energy peak located in the range of 600–1000 nm grows in going from solution to films.

TABLE 1 Molecular Weights, Yields, and Thermal Properties of Polymers

Polymer	M_n	M_w	PDI	Yield (%)	T_d (°C)
1	26,000	46,300	1.78	86	345
2	10,700	17,900	1.67	58	342
3	8,500	16,500	1.94	34	359

FIGURE 3 Cyclic voltammograms of polymer films in acetonitrile solution containing 0.1 M Bu_4NPF_6, $Ag/AgNO_3$ as the reference electrode.

−1.17 V. The onset oxidation potentials (E_{ox}), which are related with the constitution of polymers, decreased from 0.76 V for **P1** to 0.59 V for **P3**. HOMO and LUMO energy levels and bandgaps ($E_{g,ec}$) of polymers were therefore calculated according to the following equations,[33] and the results are summarized in Table 2.

$$E_{HOMO} = -e(E_{OX} + 4.71)(eV)$$

$$E_{LUMO} = -e(E_{red} + 4.71)(eV)$$

$$E_{g,ec} = -e(E_{OX}^{onset} - E_{red}^{onset})(eV)$$

The CV results illustrated that these new polymers are good candidates as donor materials. The LUMO energy levels of **P1–3** are in the range of −3.54 to −3.6 eV, which are higher than that of $PC_{61}BM$ (−4.2 eV), guaranteeing the photoinduced electrons transfer from the donor to acceptor, that is, from polymers to $PC_{61}BM$. For a clear comparison, the energy levels determined by the electrochemical method are shown in the energy level diagrams in Figure 4. **P1** has a bandgap of 1.91 eV; whereas, **P2** and **P3** show rather lower bandgap (about 1.75 eV). The optical bandgaps (E_g^{opt}) of the three polymers calculated from the absorption onset of polymer films and the $LUMO_{opt}$ energy levels calculated according to the equation: $LUMO = HOMO + E_g^{opt}$ (eV) are also summarized in Table 2. The poor agreement between the E_g^{ec} and E_g^{opt} is probably originated from the interface barrier between the polymer film and the electrode surface.[34]

FIGURE 2 Normalized UV–Vis–NIR absorption spectra of **P1–3** in (**a**) dilute $CHCl_3$ solution and (**b**) films on quartz substrates.

Electrochemical Properties

The electrochemical properties of **P1–3** were investigated by cyclic voltammetry with a standard three-electrode electrochemical cell in a 0.1 M tetrabutylammonium hexafluorophosphate ($TBAPF_6$) solution in acetonitrile at room temperature under a nitrogen atmosphere with a scanning rate of 100 mV/s. $Ag/AgNO_3$ was used as the reference electrode and a standard ferrocene/ferrocenium redox system was used as the internal standard. The CV curves of **P1–3** are shown in Figure 3 and the onset oxidation and reduction potential data are listed in Table 2. **P1–3** films showed reversible oxidation and reduction processes with similar onset reduction potentials (E_{red}) ranging from −1.11 to
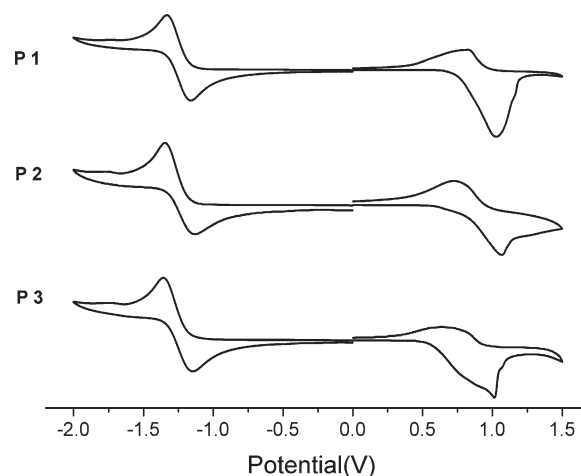
TABLE 2 Electrochemical and Optical Properties of the Polymers

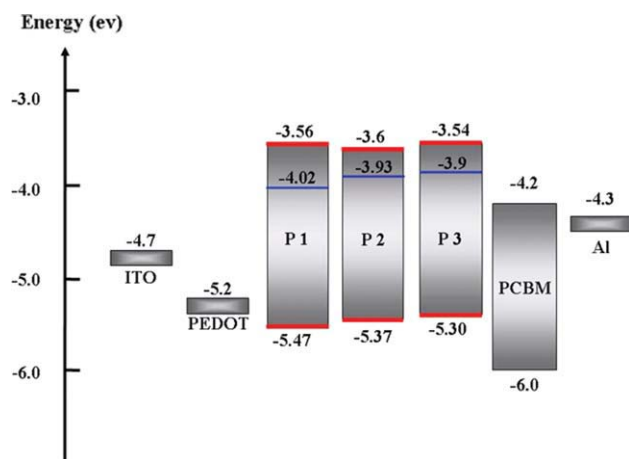| Polymer	In Solution		In Film		E_{ox} (V)/HOMO (eV)	E_{red} (V)/LUMO (eV)	$E_{g,ec}$ (eV)	$E_{g,opt}$ (eV)	$LUMO_{opt}$ (eV)
	λ_{max} (nm)	λ_{onset} (nm)	λ_{max} (nm)	λ_{onset} (nm)					
P1	700	820	746	857	0.76/−5.47	−1.15/−3.56	1.91	1.45	−4.02
P2	706	833	762	864	0.66/−5.37	−1.11/−3.60	1.77	1.44	−3.93
P3	716	872	777	883	0.59/−5.30	−1.17/−3.54	1.74	1.40	−3.9

FIGURE 4 Energy level diagrams for **P1–3**. (i) Polymer energy levels calculated from the electrochemical cyclic voltammetry results (red line); (ii) LUMO levels calculated from the absorption onset in films (blue line). [Color figure can be viewed in the online issue, which is available at www.interscience.wiley.com.]

FIGURE 5 Current-voltage characteristics for the PSCs based on the broad absorption polymer **P1–3**.

Photocurrent-Voltage Characteristics

Photovoltaic properties of **P1–3** were investigated with the device configuration of ITO/PEDOT:PSS/polymer:$PC_{61}BM$/Al. The polymer and $PC_{61}BM$ blend active layers were spin-coated from 1,2-dichlorobenzene (DCB) solution with a concentration of 7.5 mg/mL. For all polymers, the optimized ratio of polymer to $PC_{61}BM$ was 1:3 (w/w) and the optimized thickness of the active layers was about 120 nm. 1,8-Diiodooctane (DIO) was also tested as additive for the fabrication of solar cells. The use of a solvent mixture of DCB and DIO (99.5:0.5, v/v) for the fabrication of solar cell devices, only for **P1** positive effect has been achieved.

I–V characteristics of devices measured under the illumination of AM 1.5 G (100 mW/cm^2) from a solar simulator are shown in Figure 5 and the detailed results are summarized in Table 3. Although no extensive optimization work has been carried out, some of the devices have shown very promising results. Without any additive, a PCE up to 1.8% with a V_{oc} of 0.7 V, a J_{sc} of 5.25 mA, and a fill factor (FF) of 0.48 was obtained for the device based on **P2**. When using 0.5% (in volume) of DIO as an additive for the fabrication of devices, for **P1** a PCE of 2.44% was obtained. Inspection of
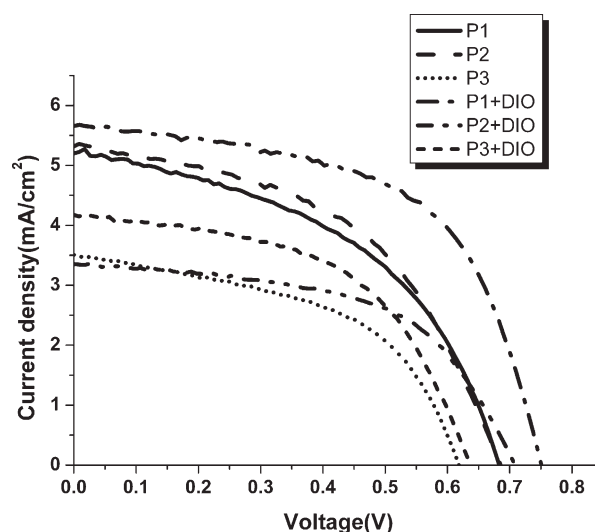
the data listed in Table 3, it is easy to find that the addition of DIO can markedly increase the PCE as well as V_{oc} and FF.

External quantum efficiency (EQE) curves of PSCs based on polymer and $PC_{61}BM$ blend films are shown in Figure 6. All the three polymers displayed broad EQE peak ranging from 300 to 870 nm. In the visible region, **P1–3** displayed different EQE curves; whereas in the long wavelength region ranging from 600 to 870 nm, they showed almost the same EQE curve shape. It is worth to note that EQE spectra are quite consistent with PCE results, in which **P2** displayed the best EQE response as well as the highest PCE. In the UV–vis–NIR absorption spectrum, **P3** displayed an intense peak in the long wavelength region of 600–870 nm; however, in the EQE spectrum, the contribution of the long wavelength absorption peak is not evident.

The AFM topography images of the polymer blend (polymer:$PC_{61}BM$ = 1:3, w/w) films spin-coated from DCB and a solvent mixture of DCB and DIO (99.5:0.5) are shown in Figure 7(a–f). The images were obtained in a surface area of 1 × 1 μm^2 by tapping mode. **P1**:$PC_{61}BM$ and **P2**:$PC_{61}BM$ blend films spin-coated from DCB exhibit smooth surfaces with root-mean-square (rms) roughness of 0.28 and 0.66 nm, respectively. **P3**:$PC_{61}BM$ (1:3, w/w) blend film shows a

TABLE 3 Photovoltaic Properties of PSCs Based on Polymer/$PC_{61}BM$ Blends

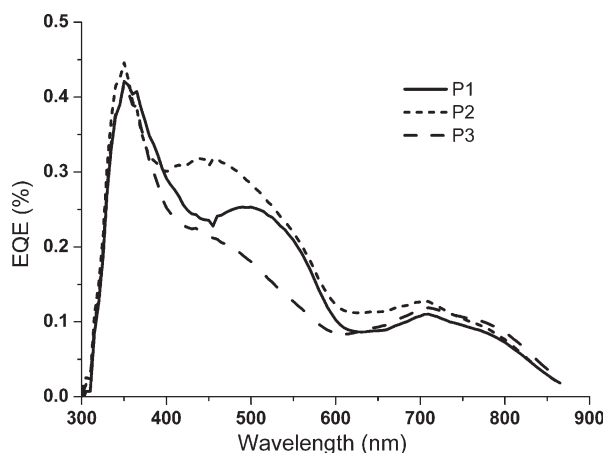| Active layer (Polymer: $PC_{61}BM$ = 1:3)	Additive Content (Volume %)	Thickness of the Active Layer (nm)	V_{OC} (V)	J_{sc} (mA/cm^2)	FF	PCE (%)
P1	no	120	0.69	5.25	0.46	1.67
P2	no	120	0.70	5.25	0.48	1.80
P3	no	120	0.65	4.25	0.48	1.32
P1	0.5	80	0.77	5.75	0.56	2.44
P2	0.5	80	0.72	3.50	0.55	1.32
P3	0.5	80	0.65	4.25	0.53	1.42

FIGURE 6 EQE curves of the PSCs based on the polymer: PC$_{61}$BM (1:3, w/w).

rough surface with rms roughness of 6.75 nm. The domain size of **P3**:PC$_{61}$BM blend film is much bigger than that of **P1**:PC$_{61}$BM and **P2**:PC$_{61}$BM blend films. It is important to note that the suitable domain size for PSCs is limited to about 10 nm,[35,36] because of the limitation of exciton diffusion length. The AFM results are therefore quite consistent with the device performances. The blend films spin-coated

from a solvent mixture of DCB and DIO (99.5:0.5) also show similar morphology. The rms roughnesses of **P1**:PC$_{61}$BM, **P2**:PC$_{61}$BM, and **P3**:PC$_{61}$BM are 0.34, 0.66, and 9.95 nm, respectively. The use of a solvent mixture (DCB:DIO = 99.5:0.5) does not show marked influence on film morphology. The constituent of polymers shows dominant influence on the morphology of blend films.

CONCLUSIONS

In conclusion, broad absorption conjugated polymers were synthesized by Suzuki–Miyaura–Schlüter polycondensation of benzo[c][1,2,5]thiadiazole containing dibromo monomer (**M1**) and [1,2,5]thiadiazolo[3,4-g]quinoxaline containing dibromo monomer (**M2**) with 9,9-dioctyl-fluoren-2,7-diboronic ester. The absorption spectra of polymers can be tuned by the feeding molar ratio of **M1** and **M2**. The broader absorption polymers, which can absorb the solar irradiation more efficiently, are promising p-type materials for heterojunction PSCs. Polymer solar devices based on these polymers (**P1–3**) are fabricated and characterized. Devices based on **P2** showed the best performance with a PCE of 1.80%, a V_{oc} of 0.7 V, a J_{sc} of 5.25 mA/cm^2, and a FF of 0.48. When a mixture of 1,2-dichlorobenzene and 1,8-diiodooctane (99.5:0.5, v/v) was used as the solvent, the PCE of devices based on **P1** increased from 1.67% to 2.44%. Nevertheless,
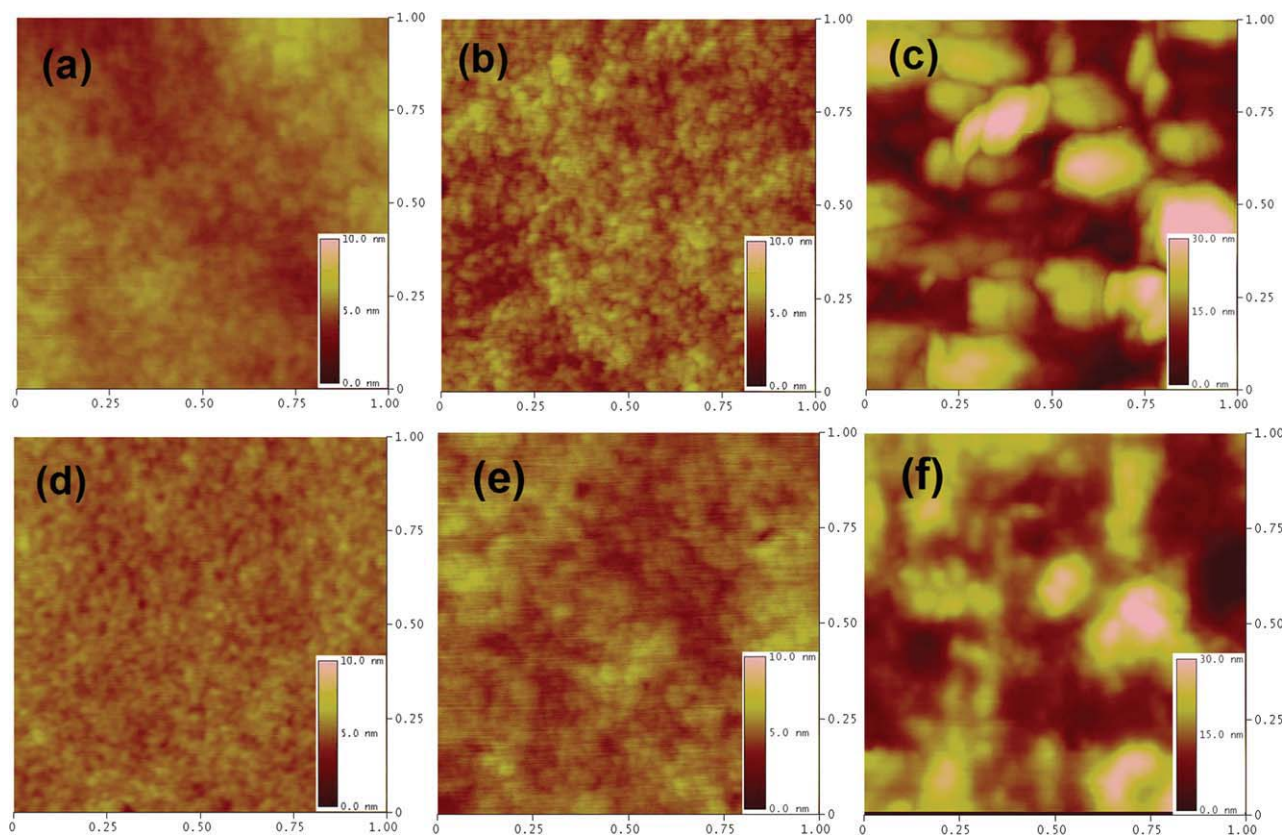

FIGURE 7 AFM images of blend films of (a) **P1**/PC$_{61}$BM (1:3, w/w), (b) **P2**/PC$_{61}$BM (1:3, w/w), and (c) **P3**/PC$_{61}$BM (1:3, w/w) spin-coated from 1,2-dichlorobenzene solution; (d) **P1**/PC$_{61}$BM (1:3, w/w), (e) **P2**/PC$_{61}$BM (1:3, w/w), (f) **P3**/PC$_{61}$BM (1:3, w/w) spin-coated from a solvent mixture of 1,2-dichlorobenzene and 1,8-diiodooctane (99.5:0.5, v/v).

these results are still not optimized, and further optimization of the device performance is in progress. This work has demonstrated that the polymerization of different monomers can afford novel broad absorption conjugated polymers for solar cells.

REFERENCES AND NOTES

1 Yu, G.; Gao, J.; Hummelen, J. C.; Wudl, F.; Heeger, A. J. Science 1995, 270, 1789.

2 Brabec, C. J.; Sariciftci, N. S.; Hummelen, J. C. Adv Funct Mater 2001, 11, 15.

3 Coakley, K. M.; McGehee, M. D. Chem Mater 2004, 16, 4533.

4 Hoppe, H.; Sariciftci, N. S. J Mater Res 2004, 19, 1924.

5 Gunes, S.; Neugebauer, H.; Sariciftci, N. S. Chem Rev 2007, 107, 1324.

6 Blouin, N.; Michaud, A.; Gendron, D.; Wakim, S.; Blair, E.; Neagu-Plesu, R.; Belletete, M.; Durocher, G.; Tao, Y.; Leclerc, M. J Am Chem Soc 2008, 130, 732.

7 Chang, Y. T.; Hsu, S. L.; Chen, G. Y.; Su, M. H.; Singh, T. A.; Diau, E. W. G.; Wei, K. H. Adv Funct Mater 2008, 18, 2356.

8 Chen, C. P.; Chan, S. H.; Chao, T. C.; Ting, C.; Ko, B. T. J Am Chem Soc 2008, 130, 12828.

9 Liang, Y. Y.; Wu, Y.; Feng, D. Q.; Tsai, S. T.; Son, H. J.; Li, G.; Yu, L. P. J Am Chem Soc 2009, 131, 56.

10 Hou, J.; Chen, H.-Y.; Zhang, S.; Li, G.; Yang, Y. J Am Chem Soc 2008, 130, 16144.

11 Qin, R.; Li, W.; Li, C.; Du, C.; Veit, C.; Schleiermacher, H.-F.; Andersson, M.; Bo, Z.; Liu, Z.; Inganäs, O.; Wuerfel, U.; Zhang, F. J Am Chem Soc 2009, 131, 14612.

12 Liang, Y.; Feng, D.; Wu, Y.; Tsai, S.-T.; Li, G.; Ray, C.; Yu, L. J Am Chem Soc 2009, 131, 7792.

13 Park, S. H.; Roy, A.; Beaupré, S.; Cho, S.; Coates, N.; Moon, J. S.; Moses, D.; Leclerc, M.; Lee, K.; Heeger, A. J Nat Photonics 2009, 3, 297.

14 Hou, J.; Chen, H.-Y.; Zhang, S.; Chen, R. I.; Yang, Y.; Wu, Y.; Li, G. J Am Chem Soc 2009, 131, 15586.

15 Kim, J. Y.; Lee, K.; Coates, N. E.; Moses, D.; Nguyen, T. Q.; Dante, M.; Heeger, A. J. Science 2007, 317, 222.

16 Van Mullekom, H. A. M.; Vekemans, J. A. J. M.; Havinga, E. E.; Meijer, E. W. Mater Sci Eng R 2001, 32, 1.

17 Tsai, F. C.; Chang, C. C.; Liu, C. L.; Chen, W. C.; Jenekhe, S. A. Macromolecules 2005, 38, 1958.

18 Svensson, M.; Zhang, F. L.; Veenstra, S. C.; Verhees, W. J. H.; Hummelen, J. C.; Kroon, J. M.; Inganäs, O.; Andersson, M. R. Adv Mater 2003, 15, 988.

19 Zhou, Q. M.; Hou, Q.; Zheng, L. P.; Deng, X. Y.; Yu, G.; Cao, Y. Appl Phys Lett 2004, 84, 1653.

20 Blouin, N.; Michaud, A.; Leclerc, M. Adv Mater 2007, 19, 2295.

21 Gadisa, A.; Mammo, W.; Andersson, L. M.; Admassie, S.; Zhang, F.; Andersson, M. R.; Inganäs, O. Adv Funct Mater 2007, 17, 3836.

22 Soci, C.; Hwang, I. W.; Moses, D.; Zhu, Z.; Waller, D.; Gaudiana, R.; Brabec, C. J.; Heeger, A. J. Adv Funct Mater 2007, 17, 632.

23 Wang, E. G.; Wang, L.; Lan, L. F.; Luo, C.; Zhuang, W. L.; Peng, J. B.; Cao, Y. Appl Phys Lett 2008, 92, 033307.

24 Muhlbacher, D.; Scharber, M.; Morana, M.; Zhu, Z. G.; Waller, D.; Gaudiana, R.; Brabec, C. Adv Mater 2006, 18, 2884.

25 Scharber, M. C.; Wuhlbacher, D.; Koppe, M.; Denk, P.; Waldauf, C.; Heeger, A. J.; Brabec, C. L. Adv Mater 2006, 18, 789.

26 Zhang, F. L.; Mammo, W.; Andersson, L. M.; Admassie, S.; Andersson, M. R.; Inganäs, O. Adv Mater 2006, 18, 2169.

27 Bundgaard, E.; Krebs, F. C. Sol Energy Mater Sol Cells 2007, 91, 954.

28 Zhang, F. L.; Bijleveld, J.; Perzon, E.; Tvingstedt, K.; Barrau, S.; Inganäs, O.; Andersson, M. R. J Mater Chem 2008, 18, 5468.

29 Perzon, E.; Wang, X.; Admassie, S.; Inganäs, O.; Andersson, M. R. Polymer 2006, 47, 4261.

30 Kenning, D. D.; Mitchell, K. A.; Calhoun, T. R.; Funfar, M. R.; Sattler, D. J.; Rasmussen, S. C. J Org Chem 2002, 67, 9073.

31 Ranger, M.; Rondeau, D.; Leclerc, M. Macromolecules 1997, 30, 7686.

32 Tolman, C. A.; Seidel, W. C.; Gerlach, D. H. J Am Chem Soc 1972, 94, 2669.

33 Sun, Q. J.; Wang, H. Q.; Yang, C. H.; Li, Y. F. J Mater Chem 2003, 13, 800.

34 Egbe, D. A. M.; Nguyen, L. H.; Hoppe, H.; Muhlbacher, D.; Sariciftci, N. S. Macromol Rapid Commun 2005, 26, 1389.35.

35 Ma, W. L.; Yang, C. Y.; Heeger, A. J. Adv Mater 2007, 19, 1387.

36 Yang, X. N.; Loos, J.; Veenstra, S. C.; Verhees, W. J. H.; Wienk, M. M.; Kroon, J. M.; Michels, M. A. J.; Janssen, R. A. J. Nano Lett 2005, 5, 579.